

Ca²⁺ released via IP₃ receptors is required for furrow deepening during cytokinesis in zebrafish embryos

KAREN W. LEE, SARAH E. WEBB and ANDREW L. MILLER*

Department of Biology, The Hong Kong University of Science and Technology, Hong Kong SAR, People's Republic of China

ABSTRACT We have previously visualized three Ca²⁺ transients, generated by release from intracellular stores, which are associated with cytokinesis during the early cell division cycles of zebrafish embryos: the furrow positioning, propagation and deepening transients. Here we demonstrate the requirement of the latter for furrow deepening, and identify the Ca²⁺ release channels responsible for generating the deepening transient. The introduction of the Ca²⁺ buffer 5,5'-dibromo-BAPTA, at an appropriate time to challenge only the deepening transient, resulted in the dissipation of this transient and an inhibition of furrow deepening. Introduction of antagonists of the inositol 1,4,5-trisphosphate (IP₃) receptor (heparin and 2-aminoethoxydiphenylborate; 2-APB) at the appropriate time, blocked the furrow deepening transient and resulted in an inhibition of furrow deepening. In contrast, antagonists of the ryanodine receptor and the NAADP-sensitive channel had no effect on either the furrow deepening transient or on furrow deepening. In addition, microinjection of IP₃ led to the release of calcium from IP₃-sensitive stores, whereas the introduction of caffeine or cADPR failed to induce any increase in intracellular Ca²⁺. Our new data thus support the idea that Ca²⁺ released via IP₃ receptors is essential for generating the furrow deepening transient and demonstrate a requirement for a localized cytosolic Ca²⁺ rise for the furrow deepening process. We also present data to show that the endoplasmic reticulum and IP₃ receptors are localized on either side of the cleavage furrow, thus providing the intracellular Ca²⁺ store and release mechanism for generating the deepening transient.

KEY WORDS: Ca²⁺, IP₃ receptor, furrow deepening, cytokinesis, zebrafish

Introduction

The involvement of Ca²⁺ in cytokinesis has been the subject of much experimentation and debate over the last 30 years (reviewed in Rappaport, 1971; 1986; 1996; Mabuchi, 1986; Hepler, 1989; 1992; 1994; Salmon, 1989; Conrad and Schroeder, 1990; Satterwhite and Pollard, 1992; Fishkind and Wang, 1995; Silver, 1996). Its exact role, however, is still somewhat unclear even in the large embryos of certain fish and amphibians where the main cytokinetic steps are far easier to resolve (both temporally and spatially) than in smaller embryos and tissue culture cells.

It has been previously shown, using zebrafish (*Danio rerio*), medaka fish (*Oryzias latipes*) and frog (*Xenopus laevis*) embryos, that the sequence of events that are involved in cytokinesis include: (1) The transmission of the furrow positioning signal from the mitotic apparatus to the cell surface, (2) The propagation of the positioned cleavage furrow across the cell surface, (3) The deepening of the cleavage furrow in order to separate the daughter cells, and (4) The zipping-up or apposition of the daughter cells following separation.

Several reports have suggested that these cytokinetic events may each involve distinct but perhaps interconnected localized Ca²⁺ transients. In fish embryos, furrow propagation, deepening and zipping transients were first visualized in dividing medaka embryos (Fluck *et al.*, 1991). Following this, three separate groups reported furrow positioning, propagation and deepening signals during the first few cell divisions of zebrafish embryos (Chang and Meng, 1995; Webb *et al.*, 1997; Créton *et al.*, 1998). Localized increases in [Ca²⁺]_i have also been observed during cytokinesis in *Xenopus* embryos. Muto *et al.* (1996) visualized localized Ca²⁺ waves spreading along the first furrow after cleavage furrow formation. In addition, most recently Noguchi and Mabuchi (2002) reported the presence of not one, but two distinct Ca²⁺ waves during the first cleavage in *Xenopus*. They suggested that the first might be the counterpart of the furrow deepening transient observed in zebrafish and medaka, and that the

Abbreviations used in this paper: 2-APB, 2-aminoethoxydiphenylborate; DBB, 5,5'-dibromo-BAPTA; ER, endoplasmic reticulum; IP₃, inositol 1,4,5 triphosphate.

*Address correspondence to: Dr. Andrew L. Miller. Department of Biology, The Hong Kong University of Science and Technology, Clear Water Bay, Hong Kong SAR, PRC. Fax: +852-2358-1559. e-mail: almill@ust.hk

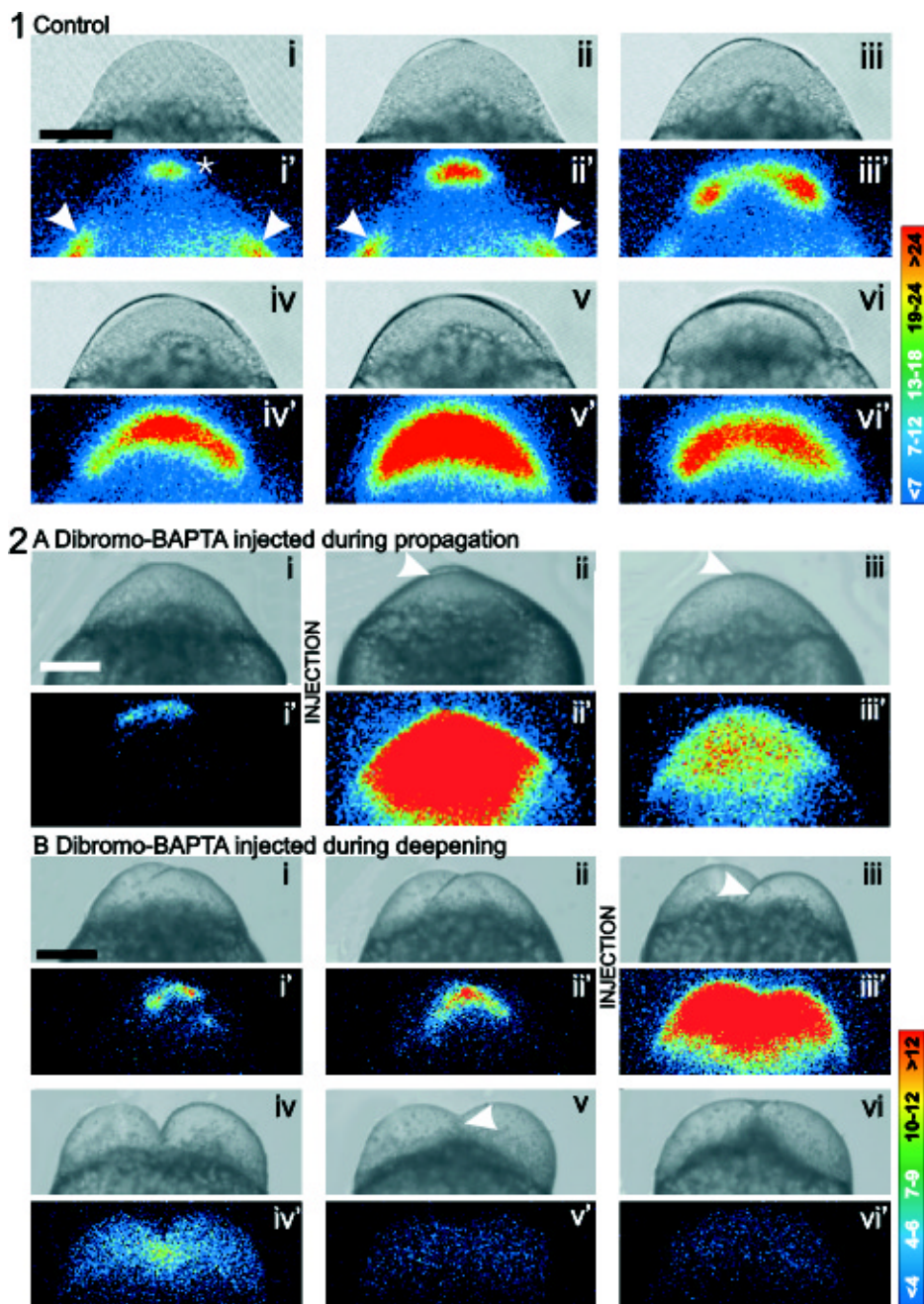


Fig. 1. Representative sequence of images from an aequorin-loaded embryo illustrating the normal changes in intracellular free Ca^{2+} during the first cell division. The embryo is in an axial orientation (Webb et al., 1997). The luminescent images (pseudocolor panels, labeled i' to vi') represent 60 s of accumulated light. A bright-field image (panels i to vi) was grabbed just prior to each luminescent image. Images were obtained as follows: (i) during the furrow positioning signal (see asterisk); at the (ii) start and (iii) end of the furrow propagation signal; at the (iv) start and (v) end of the furrow deepening signal and (vi) during furrow apposition of the first cell division cycle. Color scale indicates luminescence flux in photons per pixel. Scale bar is 200 μm . Figure modified from Webb et al. (1997). Arrowheads in panels i' and ii' indicate Ca^{2+} elevations associated with ooplasmic segregation (Leung et al., 1998).

Fig. 2. Representative sequences of images from aequorin-loaded embryos illustrating the changes in intracellular free Ca^{2+} after injection with DBB following the protocols illustrated in (A) Fig. 3A and (B) Fig. 3B. The luminescent images (pseudocolor panels, labeled in A i' to iii' and in B i' to vi') represent 60 s of accumulated light. A bright-field image (in A labeled i to iii and in B labeled i to vi) was grabbed just prior to each luminescent image. Images in (A) were collected with the embryo in an axial orientation as follows: (i and i') during the propagation signal and then (ii and ii') immediately and (iii and iii') ~20 min after the DBB injection. Arrowhead in panel ii shows the propagating furrow while the arrowhead in panel iii shows the regressed furrow. Images in (B) were obtained as follows: (i and i') during the propagation and (ii and ii') during the deepening signal of the first cell division. To facilitate the observation of furrow regression, images iii to vi show the embryo in a facial orientation and were obtained as follows: (iii and iii') immediately, (iv and iv') 15 min, (v and v') 30 min and (vi and vi') 45 min after the DBB injection. Arrowhead in panel (iii) indicates the deepening furrow whilst the arrowhead in panel (v) indicates the regressing furrow. Scale bar represents 200 μm .

second might be involved in the apposition of the two daughter blastomeres after furrow deepening has been completed.

In all the reports described above, the authors attempted to explore the function and developmental significance of the Ca^{2+} transients, as well as their mechanism of generation, by introducing Ca^{2+} buffers or antagonists of the various Ca^{2+} release channels thought to be involved. However, the timing of their introduction as well as their rate of spread within an embryo is crucial to understanding what effect they have on the generation of a particular transient, and the developmental significance of blocking or modulating that transient. For example, it has been shown that when dividing *Xenopus* embryos are injected with members of the BAPTA family of Ca^{2+} buffers (Pethig et al., 1989), the timing of the injection is

critical; if the buffer is introduced too early then it blocks karyokinesis rather than cytokinesis, and the embryos fail to divide (Miller et al., 1993; Snow and Nuccitelli, 1993). If, however, it is introduced immediately after the completion of karyokinesis, but before the onset of cytokinesis, then furrow positioning is affected (Miller et al., 1993).

In many of these reports, however, the protocols followed with regards to when the buffer or antagonist was introduced, makes it hard to distinguish which of the possible downstream cytokinetic Ca^{2+} transients were affected. Did just one or all the steps in the cytokinesis process (i.e., furrow positioning, propagation, deepening and apposition) have a Ca^{2+} -dependency? Using zebrafish embryos, Webb et al. (1997) focussed their attention on the propagation

transient, and waited until the furrow had been positioned on the blastodisc surface (by observing either the appearance of the furrow on the surface or the Ca²⁺ transient associated with this event) before they introduced 5,5'-dibromo-BAPTA. These experiments clearly indicated a Ca²⁺-requirement for furrow propagation in these embryos. However, without furrow propagation there can be no furrow deepening and so the Ca²⁺-dependency of the subsequent deepening process was still unclear.

Here, in a continuation of our work on cytokinesis in zebrafish, we demonstrate that a localized elevation of cytosolic Ca²⁺ is also essential for furrow deepening and show that the Ca²⁺ generating the deepening transient is released via inositol 1,4,5-trisphosphate receptors (IP₃Rs). We also present data indicating that the endoplasmic reticulum (ER) and IP₃Rs are both localized on either side of the cleavage furrow, thus providing additional supporting evidence for the intracellular calcium source and release mechanism responsible for generating the deepening transient.

Results

Sequence of Ca²⁺ transients accompanying cytokinesis in control embryos

The normal sequence of Ca²⁺ transients that accompany cytokinesis of the first cell division are shown in Fig. 1. This representative embryo shows the transients from an axial view (Webb *et al.*, 1997). A localized elevation of Ca²⁺, the furrow positioning signal (see asterisk in Fig. 1, panel i'), is observed just prior to the first physical sign of the cleavage furrow appearing on the blastodisc surface (see Fig. 1, panel i). After the furrow is positioned, two slow subsurface Ca²⁺ waves, (the furrow propagation signal; see Fig. 1, panels ii' and iii'), accompany the lateral extension of the furrow (see Fig. 1, panels ii and iii) and move outward toward the edge of the blastodisc. As the two wave fronts approach the edge of the blastodisc, the furrow deepening signal appears at the apex of the blastodisc where the positioning signal was first observed (see Fig. 1, panel iv'). The deepening signal moves both outward to the edge of the blastodisc and downward to the bottom of the blastodisc (see Fig. 1, panel v'). This deepening signal then begins to diminish from the apex outward (see Fig. 1, panel vi') and by the end of cytokinesis the localised Ca²⁺ elevation returns to precleavage resting levels. This is described in further detail in Webb *et al.* (1997).

The effect of 5,5'-dibromo-BAPTA on furrow deepening and apposition

A representative example (n = 3) to show the effect of the weak (K_D = 1.5 μM) Ca²⁺ buffer, 5,5'-dibromo-BAPTA (DBB), on the

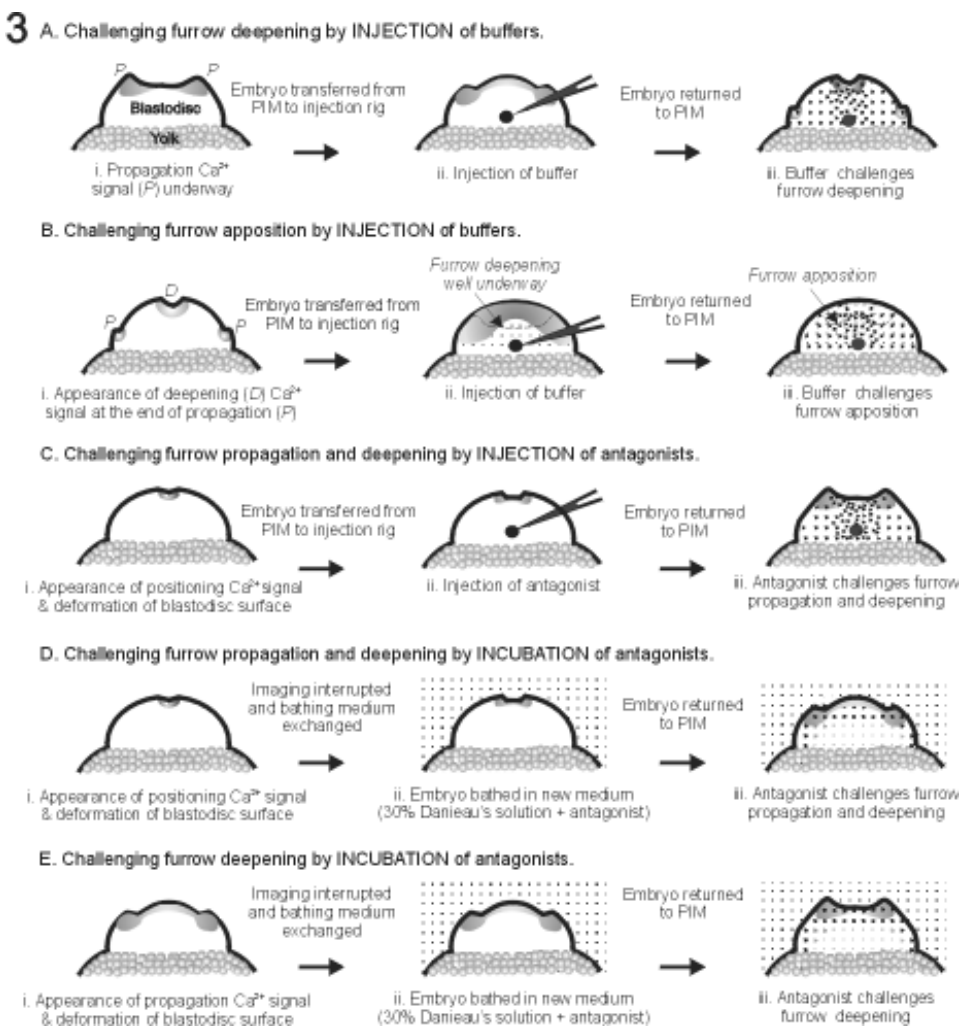


Fig. 3. Schematic representation of the experimental protocols used for challenging the different aspects of the cytokinetic process (i.e., furrow propagation, deepening and apposition) with Ca²⁺ channel antagonists, agonists and buffers.

deepening Ca²⁺ signal is illustrated in Fig. 2A. Following the timing protocols described in Fig. 3A, DBB was injected into the blastodisc of the embryo to reach a final cytosolic concentration of ~260 μM. The luminescent images (see Fig. 2A, panels ii' and iii') clearly show that the buffer delocalizes the Ca²⁺ transient, and the corresponding bright-field images show that the deepening furrow (see arrowhead in panel ii) eventually regresses (see arrowhead in panel iii). When the same final concentration (i.e., ~260 μM) of 5,5'-dimethyl-BAPTA (DMB; K_D = 0.15 μM) is introduced, however, it has no effect on the deepening transient and embryos divide and develop normally (n = 3; data not shown). The effect of DBB on furrow apposition is also illustrated (see Fig. 2B). In this representative embryo (n = 4) the buffer was injected following the injection protocol illustrated in Fig. 3B. The luminescent images (see Fig. 2B, panels iii' to vi') again show that the buffer delocalizes the Ca²⁺ transients and the corresponding bright-field images show that although the furrow deepens (see arrowheads in Fig. 2B, panels iii and v), apposition of the daughter cells is abnormal and the furrow again eventually regresses (Fig. 2B, panel vi).

Effects of Ca²⁺ channel antagonists on propagation and deepening transients

The effects of different Ca²⁺ channel antagonists on the cytokinetic Ca²⁺ transients during the first cell division cycle are shown in Figs. 4 to 6.

IP₃-sensitive channel

Figure 4A illustrates a representative control embryo (n = 5) and shows the typical pattern of luminescence observed to

accompany furrow positioning, propagation and deepening of the first cell division cycle. Figure 4B shows an example (n = 6) of an embryo injected with heparin, following the protocol described in Fig. 3C. The propagation transient (see Fig. 4B panel ii') extends normally to the edge of the blastodisc, but the deepening transient clearly does not progress down through the blastodisc to the yolk cell (compare the heparin-treated embryo, Fig. 4B panel iii' with the control, Fig. 4A, panel iii'). The corresponding bright-field images show that the extent of the furrow deepening in the

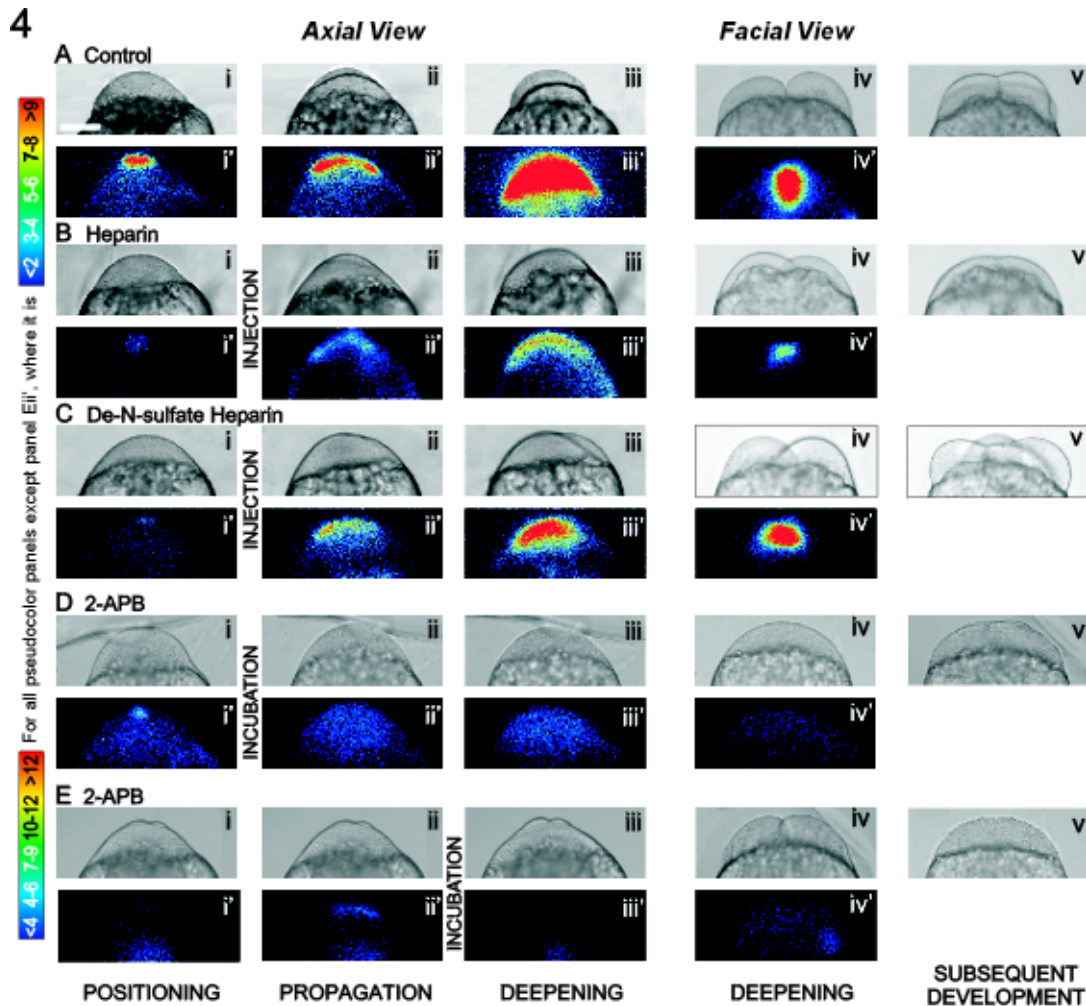


Fig. 4. Effect of IP₃ receptor antagonists on the propagation and deepening Ca²⁺ transients. Representative sequence of images from aequorin-loaded embryos illustrating the changes in intracellular free Ca²⁺ during the first two cell division cycles when (A) raised under normal conditions; after injection with (B) heparin or (C) de-N-sulfate heparin, or incubated with 2-APB to challenge (D) the propagation and deepening transients and (E) the deepening transient alone following the protocols illustrated schematically in Fig. 3. The luminescent images (pseudocolor panels, labeled i' to iv') represent 60 s of accumulated light. A bright-field image (i to iv) was grabbed just prior to each luminescent image. In addition, a bright-field image (v) was grabbed at ~60 min post-fertilization when the embryos should be at the 4-cell stage. Images i to iii show the embryos in an axial orientation and were obtained as follows: (i and i') during the positioning signal that accompanies the first appearance of the furrow arc; then during (ii and ii') the propagation and (iii and iii') the deepening signals of the first cell division. Images iv and iv' show a bright-field facial view of the first cell division and a pseudocolor facial view of the deepening signal, respectively. The concentrations of the channel antagonists used are listed in Table 1. Color scale indicates luminescent flux in photons per pixel. Scale bar represents 200 μm.

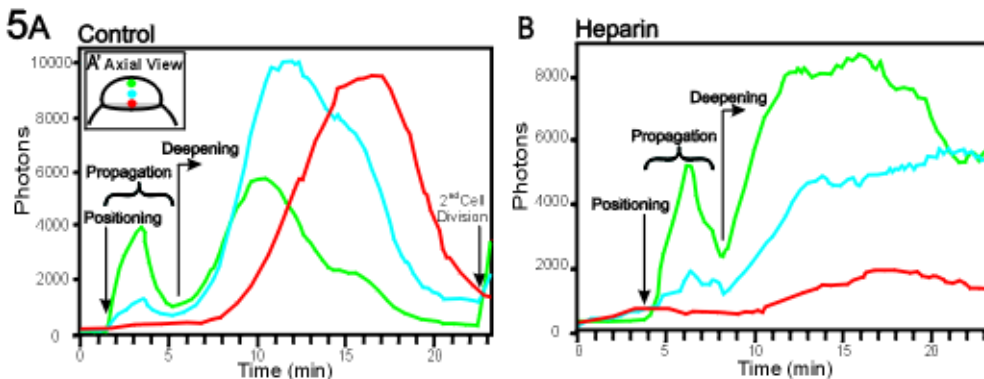


Fig. 5. Analysis of luminescence profiles during positioning, propagation and deepening of the first cell division in aequorin-loaded embryos, that were either (A) raised under normal conditions, or (B) injected with heparin during furrow positioning of the first cell division. With the embryos in an

axial orientation, the profiles were obtained from 3 regions of the blastodisc shown in A': apex (green trace), middle (blue trace) and bottom (red trace) using the Count Rate Plot function in the IpdWin 95 software. Each profile shows the relative number of photons collected in a 120 s window.

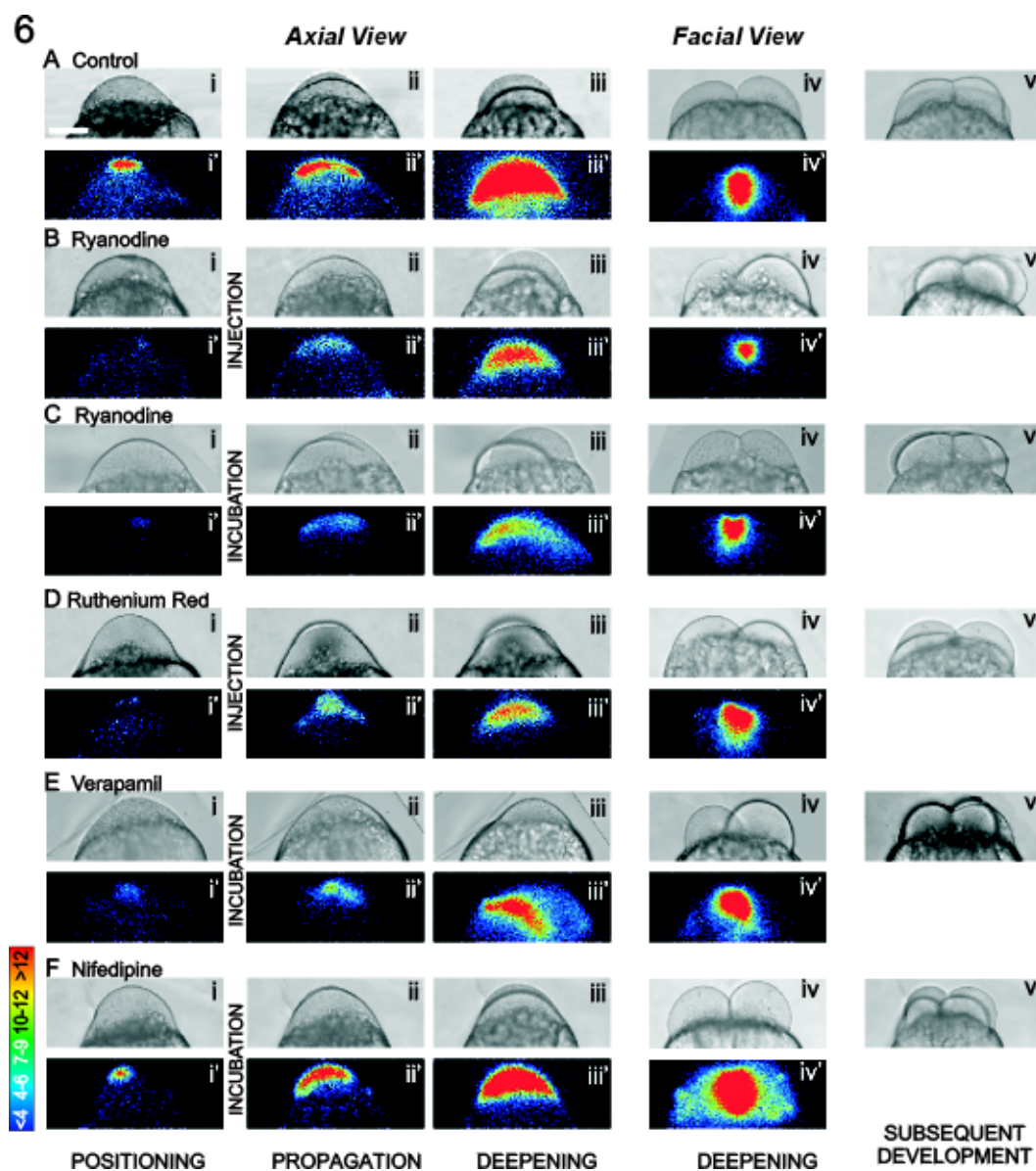
heparin-treated embryo is also significantly less than in the untreated control (compare Figs. 4B, panel iv and 4A, panel iv). The limited extent of deepening that does occur in the heparin-treated embryos eventually regresses (see Fig. 4B, panel v). Figure 4C shows a representative example (n = 8) of an embryo injected with de-N-sulfated heparin. This inactive form of heparin has no effect on the transients and the embryo continues to divide normally during subsequent cell divisions (see Fig. 4C, panel v). Figure 4D shows a representative embryo (n = 14) incubated with the cell permeable IP₃-sensitive channel antagonist, 2-aminoethoxydiphenylborate (2-APB), following the protocol described in Fig. 3D, to challenge the propagation transient. The propagation transient (see Fig. 4D, panel ii') is completely abolished after incubation (compared to the control, Fig. 4A, panel ii'). The corresponding bright-field image shows that the furrow does not propagate to the edge of the blastodisc. Figure 4D panels iii' and iv' also clearly show that the deepening transient is also completely abolished. However, as mentioned

previously, without furrow propagation there can be no furrow deepening. Thus in order to study the effect of 2-APB on the furrow deepening transient alone, 2-APB was applied after the furrow propagation transient was over, following the protocol described in Fig. 3E. Figure 4E shows an example (n = 7) of an embryo where incubation with 2-APB challenges the deepening transient. Figure 4E, panels iii' and iv' show that 2-APB completely inhibits the deepening transient, while the associated bright-field images (panels iii and iv) show that although deepening was initiated, the furrow does not progress down through the blastodisc to the yolk cell. The furrow eventually regresses and the embryo remains at the one-cell stage (Fig. 4E, panel v).

Effect of heparin on propagation and deepening profiles

We analysed the relative profiles of luminescence along the first cleavage furrow during furrow propagation and deepening. Figure 5A shows the profiles generated by the control embryo in Fig. 4A

Fig. 6. Effect of ryanodine receptor and NAADP-sensitive channel antagonists on the propagation and deepening Ca²⁺ transients. Representative sequence of images from aequorin-loaded embryos illustrating the changes in intracellular free Ca²⁺ during the first two cell division cycles when (A) raised under normal conditions; (B) either injected or (C) incubated with ryanodine, injected with (D) ruthenium red and incubated either with (E) verapamil and (F) nifedipine, following the protocols illustrated schematically in Fig. 3. The luminescent images (pseudocolor panels, labeled i' to iv') represent 60 s of accumulated light. A bright-field image (i to iv) was grabbed just prior to each luminescent image. In addition, a bright-field image (v) was grabbed at ~60 min post-fertilization when the embryos should be at the 4-cell stage. Images i to iii show the embryos in an axial orientation and were obtained as follows: (i and i') during the positioning signal that accompanies the first appearance of the furrow arc; then during (ii and ii') the propagation and (iii and iii') the deepening signals of the first cell division. Images iv and iv' show a bright-field facial view of the first cell division and a pseudocolor facial view of the deepening signal, respectively. The concentrations of the channel antagonists used are listed in Table 1. Color scale indicates luminescent flux in photons per pixel. Scale bar represents 200 μm.

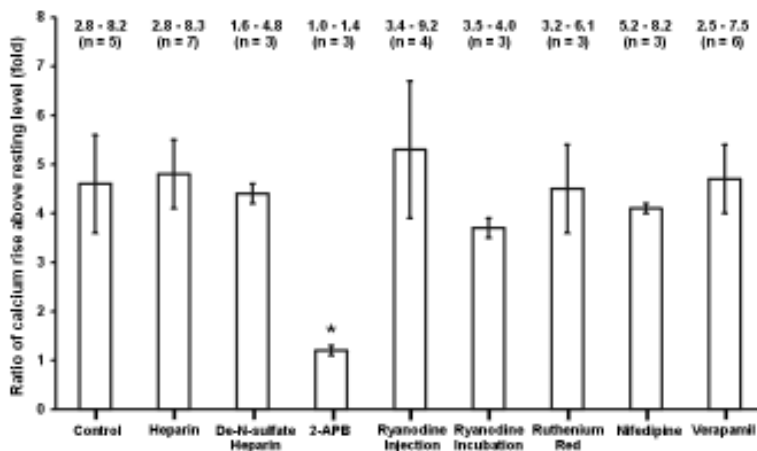


(panels i' to iii'). It indicates that whilst the positioning and propagation transients are restricted to the outer cortex of the blastodisc, the deepening transient spreads down through the blastodisc toward the non-dividing yolk cell. The ingressing furrow accompanies the slow moving Ca^{2+} wave thus serving to cut the blastodisc in two. Figure 5B shows the profiles generated by the heparin-treated embryo in Fig. 4B (panels ii' and iii'). Whereas the propagation transient appears to occur as normal in the blastodisc cortex, the deepening transient and its accompanying ingressing furrow are this time also restricted to the outer regions of the blastodisc and never penetrate down toward the yolk cell. This analysis supports the suggestion that Ca^{2+} release via IP_3Rs plays a crucial role in the latter stages of furrow deepening.

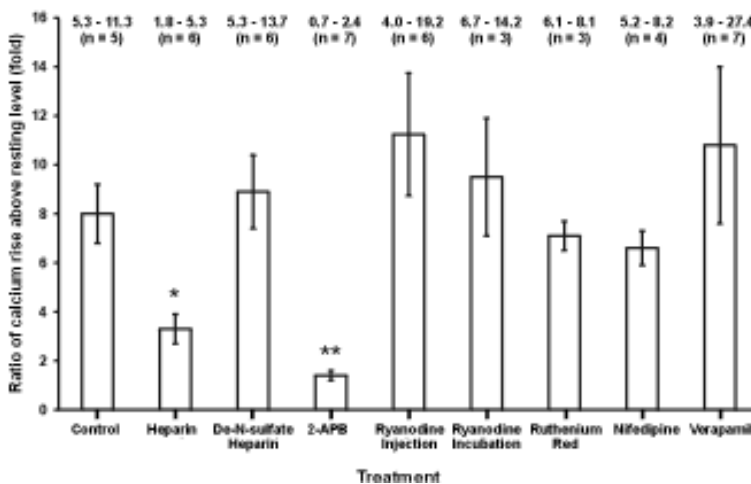
Ryanodine-sensitive channel

Figure 6A illustrates the control embryo again for comparative purposes. Figures 6 B,C show representative embryos injected ($n = 15$) and incubated ($n = 5$) and with ryanodine, respectively following the protocols illustrated in Fig. 3 C,D, respectively. Figure 6D shows a representative embryo injected with ruthenium red ($n = 14$) following the protocol described in Fig. 3C. Neither of these antagonists have an effect on either the propagation or deepening transients, and furrows propagate and deepen normally during the early cell division cycles (see Figs. 6B to D, panels v).

7 A Furrow propagation transient



B Furrow deepening transient



NAADP-sensitive channel

Figures 6 E,F show examples of embryos treated with high concentrations (see Materials and Methods) of the L-type calcium channel antagonists, verapamil ($n = 25$) and nifedipine ($n = 12$), respectively following the protocols illustrated in Fig. 3D. At such concentrations, these compounds have been reported to act as antagonists of NAADP-sensitive channels (Genazzani *et al.*, 1996, 1997). Neither of these antagonists have an effect on the propagating and deepening cytokinesis transients or the process of cytokinesis itself, and treated embryos develop normally (see Figs. 6 E,F panels v).

The results illustrated in Figs. 4 to 6 are summarized in Table 1 along with the antagonist concentrations (or ranges) used. Control embryos incubated in equivalent concentrations of DMSO ($n = 38$) or injected with injectate dilution buffer ($n = 8$) alone, all develop normally and generate normal patterns of cytokinetic Ca^{2+} transients (data not shown).

Range of elevated Ca^{2+} during propagation and deepening transients

Figure 7 displays the mean fold Ca^{2+} rise (\pm s.e.m.) of the furrow propagation (7A) and deepening (7B) transients above the background resting level, comparing (using Student t-test) antagonist treated (for concentrations see Table 1) with control embryos. In the case of the propagation transient, only incubation in medium containing 2-APB resulted in a significantly lower (where $P < 0.05$) fold increase in Ca^{2+} . Whereas in the case of the deepening transient, both incubation in 2-APB and injection of heparin resulted in a significantly lower fold increases in Ca^{2+} rise (where $P < 0.001$ and $P < 0.01$ respectively). Figure 7 also indicates the range of values calculated for the fold Ca^{2+} rises and the number of experiments carried out for each antagonist (or control).

Release of calcium by various Ca^{2+} channel agonists

Figure 8 shows the release of calcium in the blastodisc by introducing various calcium channel agonists into aequorin-loaded embryos. Figures 8 A,B show representative examples of embryos that were injected with IP_3 ($n = 15$) and NAADP ($n = 7$), respectively, prior to the appearance of the cleavage furrow at the blastodisc surface, and show that Ca^{2+} is released immediately after agonist introduction. Figures 8 C,D show embryos either incubated in caffeine ($n = 5$) or injected with cyclic ADP ribose ($n = 11$),

Fig. 7. Effect of Ca^{2+} channel antagonists on the ratio of Ca^{2+} rise above resting level for (A) the propagation and (B) the deepening transients. The data presented in the histograms are expressed as means \pm s.e.m., while the numbers above each bar show the range of values calculated and the number of imaging experiments carried out for each antagonist (or control). Student t-tests were performed and show that for the propagation transient (A), the ratio of Ca^{2+} rise above resting for the 2-APB-treated embryos (*) was significantly lower than the control at $P < 0.05$, whilst for the deepening transient (B), the ratio of Ca^{2+} rise above resting for the heparin (*) and 2-APB (**) -treated embryos, was significantly lower than the control at $P < 0.01$ and $P < 0.001$, respectively. The concentrations of the channel antagonists used are listed in Table 1.

Fig. 8. Use of Ca²⁺ channel agonists to determine the source of cytotkinetic Ca²⁺ transients. Representative examples of aequorin-loaded embryos illustrating the changes in intracellular free Ca²⁺ after introduction of (A) IP₃; (B) NAADP; (C) caffeine; and (D) cyclic ADP ribose. The luminescent images (pseudocolor panels, labeled i' and ii') represent 60 s of accumulated light. A bright-field image (panels i and ii) was grabbed just prior to each luminescent image. Images were obtained as follows: (i) before and (ii) after the introduction of the agonist before the first cell division cycle. Color scale indicates luminescent flux in photons per pixel. The asterisks represent the positioning calcium transient and WS represents the wound signal after injection. The concentrations of the channel agonists used are listed in Table 2. Scale bar represents 200 μm.

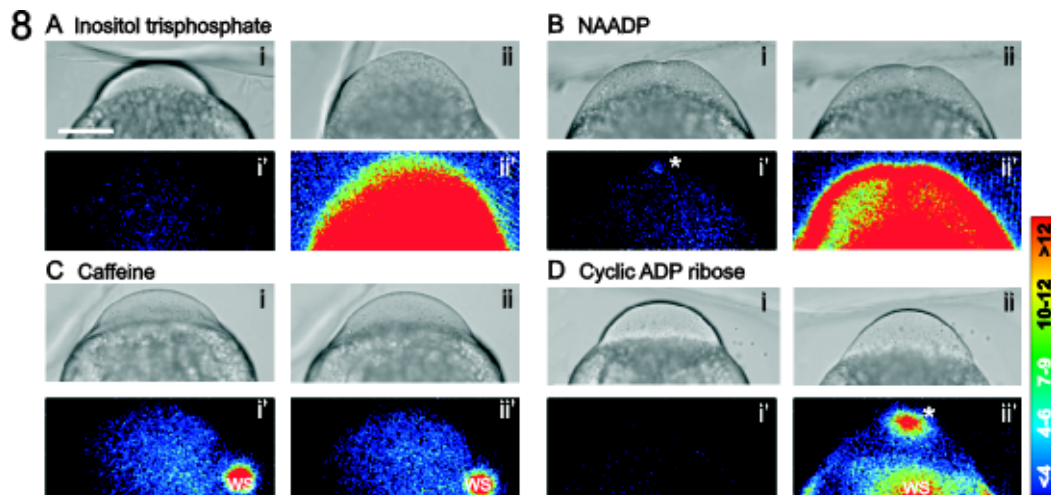
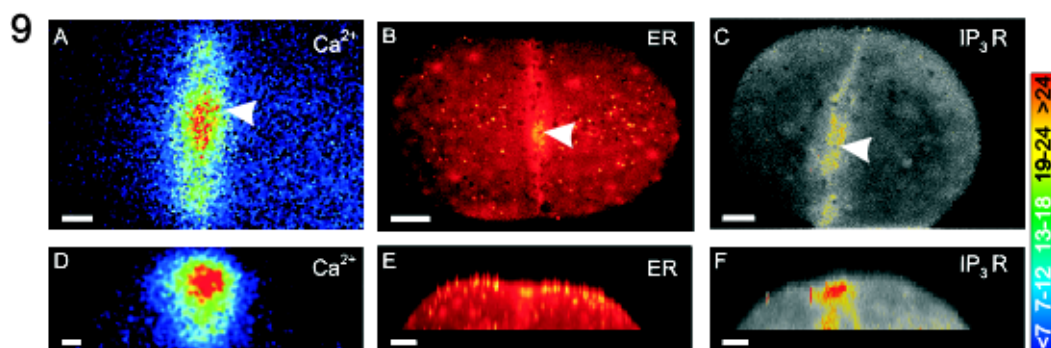


Fig. 9. Localization of Ca²⁺, the ER and IP₃Rs in the furrow during deepening of the first division cycle. Representative examples of embryos viewed (A-C) from the top and (D-F) from a facial view to show the localization of Ca²⁺ (A,D), the ER (B,E) and IP₃Rs (C,F) in the furrow (arrowheads) during deepening of the first division cycle. (A,D) Luminescent images represent 60 s of accumulated light. Color scale indicates luminescent flux in photons per pixel. (B,C,E,F) Stacks of confocal z-sections (2.5 μm step) of the deepening cleavage furrow taken through the top of the embryo are projected as single images (B,C) viewed in the same orientation as the sections were acquired (i.e., from a top view) and (E,F) viewed when the projected sections were rotated 90°. All scale bars represent 50 μm (A-D) both horizontally and vertically and (E,F) horizontally alone.



respectively. Neither of these agonists have an effect on releasing calcium via the ryanodine-sensitive calcium channel. The results shown in Figure 8 and the concentrations of agonists introduced are summarized in Table 2.

Visualizing the distribution of Ca²⁺, ER and IP₃ receptors during furrow deepening

Figure 9 shows three representative embryos to demonstrate the pattern of intracellular free Ca²⁺ from a top (A) and facial (D) view (n = 8); the localization of the ER from the top (B) and facial (E) views (n = 7); and the localization of Type 1 IP₃Rs from the top (C) and facial (F) views (n = 7). These data clearly indicate (from both orientations), that Type 1 IP₃Rs and the ER are co-localized with the domain of elevated intracellular free Ca²⁺ on either side of the deepening cleavage furrow.

TABLE 1

SUMMARY OF THE CONCENTRATIONS OF Ca²⁺ CHANNEL ANTAGONISTS USED FOR TREATING EMBRYOS AND THEIR EFFECT ON THE PROPAGATION AND DEEPENING TRANSIENTS

Ca ²⁺ Release Channel	Antagonist (* Incubation) (**Injection)	Final Antagonist Concentration	Normal Propagation Transient	Normal Deepening Transient	Ref.
IP ₃ Receptor	*2-APB	500 μM	No	No	Bilmen & Michelangeli, 2002
	**Heparin	130-400 μg/ml	Yes	No	Chang & Meng, 1995
	**De-N-sulfated Heparin	130-1050 μg/ml	Yes	Yes	
	Heparin (inactive control)				
Ryanodine Receptor	**Ryanodine	80-120 μM	Yes	Yes	Ehrlich <i>et al.</i> , 1994
	*Ryanodine	500 μM	Yes	Yes	
NAADP-Sensitive Channel	**Ruthenium red	80-110 μM	Yes	Yes	Ozawa & Nishiyama, 1997
	*Nifedipine	200 μM	Yes	Yes	Genazzani <i>et al.</i> , 1996
	*Verapamil	250 μM	Yes	Yes	

TABLE 2

SUMMARY OF THE CONCENTRATIONS OF Ca²⁺ CHANNEL AGONISTS USED FOR TREATING EMBRYOS TO RELEASE CALCIUM FROM INTRACELLULAR STORES

Ca ²⁺ Release Channel	Agonist (* Incubation) (**Injection)	Final Agonist Concentration	Ca ²⁺ Release
IP ₃ Receptor	**IP ₃	0.2 - 33 μM	Yes
Ryanodine Receptor	*Caffeine	500 μM	No
	**cADP Ribose	10 - 30 μM	No
NAADP-Sensitive Channel	**NAADP	60 - 330 nM	Yes

Discussion

Requirement of elevated Ca^{2+} for both furrow deepening and apposition

Several groups have previously reported the presence of three distinct Ca^{2+} transients that accompany the first cell division in zebrafish embryos: the furrow positioning, propagation and deepening transients (Chang and Meng, 1995; Webb *et al.*, 1997; Créton *et al.*, 1998; Chang and Lu, 2000). In this current study we focussed on the propagation and deepening Ca^{2+} transients in order to characterize further their mode of generation as well as the requirement of the latter in the cytokinetic process. The furrow propagation transient has been shown to take the form of two slow linear Ca^{2+} waves that propagate from the furrow-positioning transient at the apex of the blastodisc, out towards its edges at a velocity of approximately 0.5 $\mu\text{m}/\text{sec}$. The extending furrow accompanies these slow Ca^{2+} waves, and also propagates out towards the edges of the blastodisc at a similar velocity. The requirement of the slow Ca^{2+} waves for furrow propagation has been previously demonstrated by introducing the Ca^{2+} buffer 5,5'-dibromo-BAPTA (DBB) into the blastodisc as soon as the furrow is positioned (Webb *et al.*, 1997). The buffer served to dissipate the slow linear Ca^{2+} waves and resulted in the arrest and eventual regression of the extending furrow. In these experiments, the timing of the introduction of the buffer was such that it could not be effecting a Ca^{2+} transient prior to the initiation of furrow propagation, such as furrow positioning (Webb *et al.*, 1997; Chang and Lu, 2000) or some Ca^{2+} -dependent step during karyokinesis, such as nuclear envelop breakdown, or the metaphase anaphase transition (Créton *et al.*, 1998). However, furrow deepening cannot occur if furrow propagation is arrested and the furrow then regresses. Thus, the requirement for elevated Ca^{2+} in the deepening process was still uncertain. Here we show that by careful timing (outlined in Fig. 3 A,B) of the introduction of an appropriate concentration of DBB, it is also possible to demonstrate the Ca^{2+} dependency of the deepening furrow as well as the subsequent apposition of the daughter cells. If DBB is introduced as the propagation Ca^{2+} wave is about to reach the edges of the blastodisc, the buffer gets to the deepening zone in time to dissipate the localized deepening transient, thus inhibiting furrow deepening. If the buffer is introduced later (i.e., injected when the deepening signal starts: see Fig. 3B), its introduction is too late to delocalize the early deepening Ca^{2+} transient and inhibit deepening, but it delocalizes the late deepening/apposition transient and prevents normal apposition of the daughter cells. Introducing a similar final cytosolic concentration of 5,5'-dimethyl-BAPTA (DMB), a buffer with a K_D value some 10-fold lower than that of DBB (0.15 μM compared to 1.5 μM respectively) was ineffective at delocalizing the deepening Ca^{2+} transient or preventing the deepening of the cleavage furrow. These results suggest that the effect of DBB is not due to some indirect effect of the buffer unrelated to binding with Ca^{2+} . They also suggest that DBB is acting to facilitate the diffusion of Ca^{2+} away from the elevated domain in the deepening furrow and thus supports previous suggestions that such injected chelators act as Ca^{2+} shuttle buffers (Speksnijder *et al.*, 1989; Miller *et al.*, 1993; Snow and Nuccitelli, 1993). These experiments support the proposal that localized domains of elevated Ca^{2+} as well as being essential for furrow propagation are also a critical requirement for furrow deepening and subsequent apposition.

Source of Ca^{2+} generating propagation and deepening transients

Once again, paying particular attention to the timing of the pharmacological challenge with respect to the stage of the cytokinetic process, we determined that neither the furrow propagation or deepening Ca^{2+} transient could be inhibited by antagonists of either ryanodine receptors (RyRs; Figs. 6B-D) or NAADP-sensitive channels (Figs. 6E-F). The furrow propagation and deepening processes were likewise unaffected by the application of these antagonists. However, introduction of the non-specific antagonists of IP_3 receptors (IP_3 Rs), heparin and 2-APB, suggested that these receptors play a significant role in generating the cytokinetic Ca^{2+} transients. Heparin injection (following the experimental protocol indicated in Fig. 3C) had no apparent effect on the propagation transient or furrow propagation across the blastodisc surface (Figs. 4B, 5B and 7A) but significantly inhibited the deepening Ca^{2+} transient and halted the deepening of the cleavage furrow (Figs. 4B, 5B and 7B). On the other hand, 2-APB incubation inhibited both the propagation transient and furrow propagation (Figs. 4D and 7A) as well as the deepening transient and furrow deepening (Figs. 4E and 7B).

The conflicting results regarding the effects of heparin and 2-APB on the generation of the furrow propagation transient might be due to several factors. Clearly, the site of localized cytokinetic Ca^{2+} release during furrow propagation is restricted mainly to the blastodisc cortex (i.e., close to the external source of membrane permeable 2-APB). Whereas, the slow diffusion rate of injected heparin (Taylor and Broad, 1998) might result in insufficient antagonist being present in the cortex during the time-window selected to challenge just the generation of the propagation transient (i.e., through following the protocol illustrated in Fig. 3C). Such factors might explain the discrepancy between the results obtained using these two IP_3 R antagonists. On the other hand, our results with regards to the inhibitory effects of heparin and 2-APB on the Ca^{2+} deepening transient (and the accompanying furrow deepening) are complimentary. We suggest that sufficient heparin is present within the deeper regions of the blastodisc through which the ingressing furrow must pass during the furrow deepening process. This inhibits the release of Ca^{2+} and thus the generation of the deepening transient, which in turn stops the deepening process and leads to eventual furrow regression.

Although heparin has traditionally been used as one of the main pharmacological inhibitors of IP_3 Rs (Chang and Meng, 1995; Stricker, 1995; Muto *et al.*, 1996; Groigno and Whitaker, 1998) it does have limitations due to multiple actions. These include activating RyRs (Bezprozvanny *et al.*, 1993), uncoupling the receptors that stimulate IP_3 formation from their G-proteins, inhibition of IP_3 3-kinase, which normally stimulates the phosphorylation of IP_3 to IP_4 , and blocking the binding of IP_4 (reviewed in Taylor and Richardson, 1991; Taylor and Broad, 1998). However, there appear to be no functional RyRs in the zebrafish blastodisc during the early cleavage period (see Figs. 8C and D) thus eliminating at least this possible complication. Unfortunately, like heparin, 2-APB is not a specific inhibitor of IP_3 receptors and is also known to have multiple actions inside cells (Bootman *et al.*, 2002). Indeed, its main antagonistic effect seems to be on Ca^{2+} entry via store-operated channels (SOCs; Gregory *et al.*, 2001) rather than on Ca^{2+} release via IP_3 Rs. In addition, only Types 1 and 3 IP_3 Rs appear to be sensitive to 2-APB while Type 2 IP_3 Rs are reported to be insensitive (Bilmen and Michelangeli, 2002; Bootman *et al.*, 2002). How-

ever, we have demonstrated previously that zebrafish embryos can generate a regular series of cytokinetic Ca²⁺ transients and divide normally (for at least the first few cell division cycles) in Ca²⁺-free medium (Webb *et al.*, 1997). This indicates that extracellular Ca²⁺ is not directly involved (even if it is refilling the ER via SOCs) in generating the cytokinetic Ca²⁺ transients and that the Ca²⁺ generating the transients is being released from intracellular stores. Furthermore, by immunohistochemistry we show that Type 1 IP₃Rs (i.e., one of the isoforms known to respond to 2-APB; Bootman *et al.*, 2002), and the ER are co-localized within the elevated level of intracellular free Ca²⁺ on either side of the cleavage furrow (see Fig. 9). Although the lateral extension of the aequorin-generated signal appears to be greater than that of the ER and IP₃R staining (compare Fig. 9A with Figs. 9B and C), this might be explained by aequorin-generated light scattering from the deepening furrow. We suggest, therefore, that in the case of the zebrafish cytokinetic Ca²⁺ transients, 2-APB was more likely to be inhibiting Ca²⁺ release via IP₃Rs, rather than inhibiting Ca²⁺ entry.

When these results are combined with those obtained from applying the antagonists of the other two Ca²⁺ release channels (i.e., the NAADP-sensitive channels and RyRs), it suggests that IP₃Rs may indeed be the release channels involved in generating these transients. A role for Ca²⁺ release via IP₃Rs during cytokinesis has also been suggested in dividing newt (*Cynops pyrrhogaster*) eggs. Microinjection of Ca²⁺ store-enriched microsomal fractions (derived from mouse cerebella and CHO cells) into these eggs induced extra cleavage furrows at the site of injection via IP₃-mediated Ca²⁺ release (Mitsuyama *et al.*, 1999).

To further support our proposition that IP₃Rs are, but RyRs and NAADP-sensitive channels are not, involved in generating the cytokinetic Ca²⁺ transients in zebrafish, we also introduced a variety of channel agonists into the blastodisc (see Fig. 8) to see if they could induce the release of calcium from their respective receptors. It is clear that injected IP₃ released Ca²⁺ via IP₃Rs and NAADP released Ca²⁺ from NAADP-sensitive channels. However, caffeine and cADP ribose did not induce any response suggesting that RyRs are either not present or are non-functional at this stage of zebrafish development. Along with the results from the antagonist injections, this provides additional compelling evidence that IP₃Rs play a key role in releasing calcium during both furrow propagation and deepening in zebrafish embryos. Introducing NAADP into the zebrafish blastodisc clearly resulted in the release of Ca²⁺ (see Fig. 8B) indicating that NAADP-sensitive channels are present in this embryo. However, the introduction of the NAADP-sensitive channel antagonists, verapamil and nifedipine, (Genazzani *et al.*, 1996, 1997) had no effect on the cytokinetic Ca²⁺ transients or cytokinesis itself, suggesting that although the NAADP-sensitive channels are present, they do not play a role in generating these Ca²⁺ signals.

Materials and Methods

Egg collection

Zebrafish (*Danio rerio*) were maintained and their fertilized eggs collected as described in detail elsewhere (Webb *et al.*, 1997). To enhance optical clarity during imaging, embryos were dechorionated by treatment with pronase (Sigma; 1 mg/ml in 30% Danieau's solution; 19.3 mM NaCl, 0.23 mM KCl, 0.13 mM MgSO₄·7H₂O, 0.2 mM Ca(NO₃)₂, 1.67 mM Hepes, pH 7.2) for several minutes at room temperature and then washed several times in 30% Danieau's solution. They were then placed in custom-made holding/viewing chambers (described in Webb *et al.*, 1997) for microinjection and subsequent imaging.

Microinjection of aequorins

The microinjection pipettes, the pressure injection system and the other protocols used for injecting embryos with aequorin are described in detail elsewhere (Webb *et al.*, 1997). Approximately 1.2 nl of recombinant *f*- or *h*-aequorin (supplied by Dr. O. Shimomura, The Photoprotein Laboratory, Falmouth, MA, USA; at 0.5-1.0% in 100 mM KCl, 5 mM MOPS, and 50 μM EDTA) was injected into the center of the embryo's yolk cell. Following microinjection, embryos were manipulated to provide a particular viewing orientation (i.e., facial, axial or top views; Webb *et al.*, 1997) and then transferred to our photon imaging microscope (PIM; Science Wares, East Falmouth, MA, USA) for data acquisition.

Data acquisition and review

Aequorin-generated and bright-field images were acquired using our custom-designed PIM, which is described in detail elsewhere (Webb *et al.*, 1997; Lee *et al.*, 1999). Images were collected using either Zeiss Fluor 10x/0.5 NA or Plan Neofluar 10x/0.3 NA objectives. At the end of data acquisition, files were downloaded into Corel DRAW 8 and PHOTO PAINT 8 (Corel Corp.) for figure preparation and presentation.

Determination of challenge time

It was important to establish protocol to ensure that the Ca²⁺ buffers, channel antagonists and agonists introduced into the blastodisc of a dividing embryo reached the propagating or deepening furrow in time to have an effect directly on the particular aspect of cytokinesis under consideration. From our previous imaging study (Webb *et al.*, 1997), we were able to obtain a good estimation of the timing of the various stages in the cytokinetic process (i.e., furrow positioning, propagation and deepening) by monitoring the appearance and progression of the associated Ca²⁺ transients. We used these, therefore, to time when the embryo should be removed from the PIM for injection. Thus, to challenge furrow propagation, deepening and apposition, embryos were removed for injection or incubation: as soon as the positioning signal appeared at the blastodisc surface (see Figs. 3C and D); as the propagation signal approached the edges of the blastodisc (see Figs. 3A and E); and when the deepening signal appeared at the apex of the blastodisc (see Fig. 3B), respectively. By following these protocols, we were confident that a particular Ca²⁺ transient was being challenged directly, rather than indirectly via an upstream Ca²⁺-sensitive step.

Calibration of injectate volume and cytosolic concentration

Micropipettes were calibrated by injecting solution under Wesson vegetable oil and measuring the diameter of the droplets produced with an eyepiece reticule (Miller *et al.*, 1994). This was always done before (and sometimes also after) each injection to ensure that a known volume had been delivered to the embryo. In order to estimate the final cytosolic concentration of injectate, the volume of each zebrafish embryo was assumed to be ~128 nl (from a dechorionated egg diameter of ~625 μm). We have previously determined the water percentage of single cell zebrafish embryos to be ~68% (Leung *et al.*, 1998). The approximate final cytosolic concentrations of the antagonists and agonists used during the experiments are given in Tables 1 and 2 respectively.

Microinjection of BAPTA buffers during furrow deepening and apposition

The need for a localized elevation of intracellular free Ca²⁺ in furrow propagation has been demonstrated previously (Webb *et al.*, 1997). Here, experiments were carried out to explore whether localized increases in intracellular free Ca²⁺ are also required for both furrow deepening and apposition of the daughter blastomeres at the end of cytokinesis. Embryos were injected with aequorin and imaged using our PIM as described above. Following the protocols described in the previous section (and see Figs. 3A and 3B), 5,5'-dibromo-BAPTA (DBB, K_D = 1.5 μM: ~0.9 nl of a 25 mM solution in 18.25 mM CaCl₂, 5 mM Hepes pH 7.0) or 5,5'-dimethyl-BAPTA (DMB, K_D = 0.15 μM: ~0.9 nl of a 25 mM solution in 10.5 mM CaCl₂, 5 mM Hepes pH 7.0) was injected into the

blastodisc and imaging then resumed. Buffers were injected to reach a final cytosolic concentration of $\sim 260 \mu\text{M}$ (see calibration factors in previous section). In the case of DBB, this concentration was shown to be 100% effective in blocking furrow deepening and apposition. For both DBB and DMB, enough CaCl_2 (i.e., 18.25 mM and 10.5 mM, respectively) was added to each buffer to set its free $[\text{Ca}^{2+}]$ at $\sim 400 \text{ nM}$, a level well above that reported for the resting level in zebrafish embryos (i.e., $\sim 60 \text{ nM}$; Créton *et al.*, 1998). Both dibromo- and dimethyl-BAPTA were obtained from Molecular Probes.

Treatment with Ca^{2+} channel antagonists

In order to identify the source and the mechanism of Ca^{2+} release used to generate the cytokinetic transients, embryos were treated with a variety of Ca^{2+} channels antagonists. The antagonists of: (1) the inositol 1,4,5 trisphosphate receptor (heparin and 2-APB), (2) the ryanodine receptor (ryanodine and ruthenium red), and (3) NAADP-sensitive calcium channel (nifedipine, and verapamil) were utilized during the study. In addition, the inactive form of heparin (de-N-sulfated heparin) was used as a heparin control. It has been reported that at low concentrations, ($<10 \mu\text{M}$) ryanodine activates the ryanodine receptor, whilst at concentrations of $>10 \mu\text{M}$ it acts as an antagonist (Ehrlich *et al.*, 1994). Here, ryanodine was used at $\sim 120 \mu\text{M}$ for microinjecting into the blastodisc and at $\sim 500 \mu\text{M}$ for incubation. Common L-type channels antagonists (i.e., nifedipine and verapamil) when used at high concentrations have been reported to inhibit the calcium release from NAADP-sensitive channels in sea urchin embryos (Genazzani *et al.*, 1996; 1997). As it has been previously established that the Ca^{2+} generating the cytokinetic transients was released from intracellular rather than extracellular Ca^{2+} stores (Webb *et al.*, 1997), these antagonists could be used to determine the possible contribution of Ca^{2+} released via NAADP-sensitive channels to the generation of cytokinetic Ca^{2+} transients without the complication of their effect on inhibiting L-type voltage-gated channels. The ruthenium red was obtained from Fluka whereas the other antagonists and the inactive heparin were obtained from Sigma. Stock solutions of heparin (H-5027; bovine intestinal mucosa sodium salt; MW 13,000; at 10 mg/ml), de-N-sulfate heparin (10 mg/ml), ruthenium red (8 mM) and the ryanodine used for the injection experiments (5 mM) were prepared in injectate dilution buffer (150 mM KCl, 5 mM Hepes, pH 7.2). The ryanodine used for the incubation experiments was prepared at 500 μM in 30% Danieau's solution. Stock solutions of 2-APB (10 mM) and nifedipine (50 mM) were prepared in dimethyl sulphoxide (DMSO), while a stock solution of verapamil (25 mM) was prepared in 30% Danieau's solution. Embryos were either injected with or incubated in the appropriate concentrations (see Table 1) of these antagonists, following the protocols described in the previous section and illustrated schematically in Fig. 3. Some embryos were also injected with injectate dilution buffer or incubated with the appropriate amount of DMSO in 30% Danieau's solution as controls.

The extent of the Ca^{2+} rise during the generation of the propagation transient in the presence or absence of channel antagonists was estimated in the following manner. The light output from a selected area of the blastodisc was measured at rest (i.e., before the occurrence of a transient) then measured again during the peak passage of the transient. Assuming that the luminescence of both *f*- and *h*-aequorin varies with $[\text{Ca}^{2+}]$ *in vivo* as it does *in vitro*, i.e., to the second power (Shimomura, 1995), we were thus able to estimate what the approximate Ca^{2+} fold rise during the transient was. This form of "self-calibration" makes experiment-to-experiment comparison of aequorin-generated data possible, where differences in aequorin loading and the ratio of spent to unspent aequorin (due to successive thawing and refreezing) injected into embryos, varies.

Treatment with Ca^{2+} channel agonists

In order to determine whether intracellular calcium is released from inositol 1,4,5-trisphosphate, ryanodine and/or NAADP-sensitive stores, the agonists of: (1) the inositol 1,4,5 trisphosphate receptor (i.e., D-myo-inositol 1,4,5-trisphosphate; IP_3), (2) the ryanodine receptor (i.e., cyclic adenosine

diphosphate ribose; cADP ribose and caffeine), and (3) the NAADP-sensitive channel (i.e., nicotinic acid adenine dinucleotide phosphate; NAADP) were utilized. Stock solutions of IP_3 (20 μM), cADP ribose (2 mM) and NAADP (0.2 mM) were prepared in injectate dilution buffer. These were injected into the blastodisc of aequorin-loaded embryos via the vegetal hemisphere just prior to the appearance of the furrow at the surface of the blastodisc. Embryos were incubated with caffeine (500 μM) in 30% Danieau's solution, again just prior to the appearance of the furrow. Caffeine solution was freshly prepared for each experiment. The NAADP was obtained from Molecular Probes while the other agonists were from Sigma.

Immunohistochemical labeling of the ER and IP_3 Receptors

Embryos were dechorionated as described above and fixed during furrow deepening of the first cell division cycle with 4% paraformaldehyde in phosphate buffered saline (PBS; Westerfield, 1994) overnight at 4°C . Fixed embryos were washed initially with PBS (>5 washes) to remove excess fixative, then with PBS containing 0.1% Tween-20 (PBT) for four 5-min washes, and finally with PBT containing 1% DMSO (PBDT) for 5 min. Embryos were then incubated in blocking buffer (PBDT containing 10% bovine serum albumin, BSA) for 2 hours after which they were incubated for one hour with either anti-calnexin (Stressgen Biotechnologies Corp.) diluted 1:100 in blocking buffer to label the ER, or else anti- IP_3 Rs (Type 1; Sigma), diluted 1:200 in blocking buffer. They were then washed extensively with PBDT containing 1% BSA (PBDT/BSA) and incubated for one hour with FITC-conjugated goat anti-rabbit IgG (H + L; Zymed Laboratories Inc.) diluted 1:100 (for the ER) or 1:500 (for the IP_3 Rs) in blocking buffer, after which they were washed extensively, again with PBDT/BSA. FITC-labelled ER and IP_3 Rs were visualized using a Bio-Rad MRC-600 laser scanning confocal microscope, equipped with a krypton/argon laser, mounted on a Zeiss Axioskop upright microscope. Images were collected using a Zeiss water immersion Achroplan 20X/0.5NA objective. Embryos were observed from an animal pole view and a z-series of confocal sections were scanned through the blastodisc to the top of the yolk cell. Figures 9B and 9C represent projected images of 21 and 25 confocal sections, respectively, to show each blastodisc from the animal pole, whereas Figs. 9E and 9F represent projected images of the confocal stacks rotated 90° to show them from a facial orientation.

Acknowledgements

We thank Drs. O. Shimomura, Y. Kishi, and S. Inouye for supplying us with the *f*- and *h*-aequorins and Prof. H.B. Peng for supplying us with the Zymed antibody. We are also grateful to Dr. A. Gallone for his recommendations concerning the antagonists, Prof. H.C. Lee for his advice on NAADP, and to Prof. M. Whitaker for his advice on the ER and IP_3 R labeling experiments. Some of the zebrafish used were supplied by the Zebrafish International Resource Center, supported by grant #RR12546 from the NIH-NCRR. This work was supported by RGC-CERG Grants HKUST 6106/01 M and HKUST6214/02M awarded to A.L.M.

References

- BEZPROZVANNY, I.B., ONDRIAS, K., KAFTAN, E., STOYANOVSKY, D.A. and EHRlich, B.E. (1993). Activation of the calcium release channel (ryanodine receptor) by heparin and other polyanions is calcium dependent. *Mol. Biol. Cell* 4: 347-52.
- BILMEN, J.G., and MICHELANGELI, F. (2002). Inhibition of the type 1 inositol 1,4,5-trisphosphate receptor by 2-aminoethoxydiphenylborate. *Cell Signaling* 14, 955-960.
- BOOTMAN, M.D., COLLINS, T.J., MACKENZIE, L., RODERICK, H.L., BERRIDGE, M.J. and PEPPIATT, C.M. (2002). 2-aminoethoxydiphenyl borate (2-APB) is a reliable blocker of store-operated Ca^{2+} entry but an inconsistent inhibitor of InsP_3 -induced Ca^{2+} release. *FASEB J.* 16: 1145-50.
- CHANG, D.C. and MENG, C. (1995). A localized elevation of cytosolic free calcium is associated with cytokinesis in the zebrafish embryo. *J. Cell Biol.* 131: 1539-1545.

- CHANG, D.C. and LU, P. (2000). Multiple types of calcium signals are associated with cell division in zebrafish embryo. *Micro. Res. Tech.* 49: 111-122.
- CONRAD, G.W. and SCHROEDER, T.E., editors (1990). Cytokinesis: Mechanisms of furrow formation during cell division. *Ann. N. Y. Acad. Sci.* 582: 1-327.
- CRÉTON, R., SPEKSNIJDER, J.E. and JAFFE, L.F. (1998). Patterns of free calcium in zebrafish embryos. *J. Cell Sci.* 111: 1613-1622.
- EHRLICH, B.E., KAFTAN, E., BEZPROZVANNAYA, S. and BEZPROZVANNY, I. (1994). The pharmacology of intracellular Ca²⁺-release channels. *TIPS* 15: 145-149.
- FISHKIND, D.J. and WANG, Y.-L. (1995). New horizons for cytokinesis. *Curr. Opin. Cell Biol.* 7: 23-31.
- FLUCK, R.A., MILLER, A.L. and JAFFE, L.F. (1991). Slow calcium waves accompany cytokinesis in medaka fish eggs. *J. Cell Biol.* 115: 1259-1265.
- GENAZZANI, A.A., EMPSON, R.M., and GALIONE, A. (1996). Unique inactivation properties of NAADP-sensitive Ca²⁺-release. *J. Biol. Chem.* 271: 11599-11602.
- GENAZZANI, A.A., MEZNA, M., DICKEY, D.M., MICHELANGELI, F., WALSETH, T.F., and GALIONE, A. (1997). Pharmacological properties of the Ca²⁺-release mechanism sensitive to NAADP in the sea urchin egg. *Br. J. Pharmacol.* 121: 1489-1495.
- GREGORY, R.B., RYCHKOV, G. and BARRITT, G.J. (2001). Evidence that 2-aminoethyl diphenylborate is a novel inhibitor of store-operated Ca²⁺ channels in liver cells, and acts through a mechanism which does not involve inositol trisphosphate receptors. *Biochem. J.* 354: 285-90.
- GROIGNO, L. and WHITAKER, M. (1998). An anaphase calcium signal controls chromosome disjunction in early sea urchin embryos. *Cell.* 92: 193-204.
- HEPLER, P.K. (1989). Calcium transients during mitosis: observations in flux. *J. Cell Biol.* 109: 2567-2573.
- HEPLER, P.K. (1992). Calcium and mitosis. *Int. Rev. Cytol.* 138: 239-268.
- HEPLER, P.K. (1994). The role of calcium in cell division. *Cell Calcium* 16: 322-330.
- LEE, K.W., WEBB, S.E. and MILLER, A.L. (1999). A wave of free cytosolic calcium traverses zebrafish eggs on activation. *Dev. Biol.* 214: 168-180.
- LEUNG, C.F., WEBB, S.E. and MILLER, A.L. (1998). Calcium transients accompany ooplasmic segregation in zebrafish embryos. *Develop. Growth Differ.* 40: 313-326.
- MABUCHI, I. (1986). Biochemical aspects of cytokinesis. *Int. Rev. Cytol.* 101: 175-213.
- MILLER, A.L., FLUCK, R.A., MCLAUGHLIN, J.A. and JAFFE, L.F. (1993). Calcium buffer injections inhibit cytokinesis in *Xenopus* eggs. *J. Cell Sci.* 106: 523-534.
- MILLER, A.L., KARPLUS, E. and JAFFE, L.F. (1994). Imaging [Ca²⁺]_i with aequorin using a photon imaging detector. In "Methods in Cell Biology" (R. Nuccitelli, Ed.), Vol. 40, pp. 305-337. Academic Press, Orlando, FL.
- MITSUYAMA, F., SAWAI, T., CARAFOLI, E., FURUICHI, T. and MIKOSHIBA, K. (1999). Microinjection of Ca²⁺ store-enriched microsomes to dividing newt eggs induces extra-cleavage furrows via inositol 1,4,5-trisphosphate-induced Ca²⁺ release. *Dev. Biol.* 214: 160-167.
- MUTO, A., KUME, S., INOUE, T., OKANO, H. and MIKOSHIBA, K. (1996). Calcium waves along the cleavage furrows in cleavage-stage *Xenopus* embryos and its inhibition by heparin. *J. Cell Biol.* 135: 181-190.
- NOGUCHI, T. and MABUCHI, I. (2002). Localized calcium signals along the cleavage furrow of the *Xenopus* egg are not involved in cytokinesis. *Mol. Biol. Cell.* 13: 1263-1273.
- OZAWA, T., and NISHIYAMA, A. (1997). Characterization of ryanodine-sensitive Ca²⁺ release from microsomal vesicles of rat parotid acinar cells: regulation by cyclic ADP-ribose. *J. Membrane Biol.* 156: 231-239.
- PETHIG, R., KUHN, M., PAYNE, R., ADLER, E., CHEN, T.H. and JAFFE, L.F. (1989). On the dissociation constants of BAPTA-type calcium buffers. *Cell Calcium* 10: 491-498.
- RAPPAPORT, R. (1971). Cytokinesis in animal cells. *Int. Rev. Cytol.* 31: 169-213.
- RAPPAPORT, R. (1986). Establishment of the mechanism of cytokinesis in animal cells. *Int. Rev. Cytol.* 105: 245-281.
- RAPPAPORT, R. (1996). Cytokinesis in animal cells. In "Developmental and Cell Biology Series" (P.W. Barlow, J.B.L. Bard, P.B. Green, and D.L. Kirk Eds.). Cambridge Univ. Press, Cambridge, UK.
- SALMON, E.D. (1989). Cytokinesis in animal cells. *Curr. Opin. Cell Biol.* 1: 541-547.
- SATTERWHITE, L.L. and POLLARD, T.D. (1992). Cytokinesis. *Curr. Opin. Cell Biol.* 4: 43-52.
- SHIMOMURA, O. (1995). Luminescence of aequorin is triggered by the binding of two calcium ions. *Biochem. Biophys. Res. Commun.* 211: 359-363.
- SILVER, R.B. (1996). Calcium, BOBs, QEDs, microdomains and a cellular decision: control of mitotic cell division in sand dollar blastomeres. *Cell Calcium* 20: 161-179.
- SNOW, P. and NUCCITELLI, R. (1993). Calcium buffer injections delay cleavage in *Xenopus laevis* blastomeres. *J. Cell Biol.* 122: 387-394.
- SPEKSNIJDER, J.E., MILLER, A.L., WEISENSEEL, M.H., CHEN, T.H. and JAFFE, L.F. (1989). Calcium buffer injections block fucoid egg development by facilitating calcium diffusion. *Proc. Natl. Acad. Sci. USA* 86: 6607-6611.
- STRICKER, S.A. (1995). Time-lapse confocal imaging of calcium dynamics in starfish embryos. *Dev. Biol.* 170: 496-518.
- TAYLOR, C.W. and BROAD, L.M. (1998). Pharmacological analysis of intracellular Ca²⁺ signalling: problems and pitfalls. *TIPS* 19: 370-375.
- TAYLOR, C.W. and RICHARDSON, A. (1991). Structure and function of inositol trisphosphate receptors. *Pharmac. Ther.* 51: 97-137.
- WEBB, S.E., LEE, K.W., KARPLUS, E. and MILLER, A.L. (1997). Localized calcium transients accompany furrow positioning, propagation, and deepening during the early cleavage period of zebrafish embryos. *Dev. Biol.* 192: 78-92.
- WESTERFIELD, M. (1994). "The Zebrafish Book: A Guide for the Laboratory Use of Zebrafish (*Brachydanio rerio*).". Univ. of Oregon Press, Eugene, OR.

Received: July 2003

Reviewed by Referees: August 2003

Modified by Authors and Accepted for Publication: August 2003

Edited by: Patrick Tam